

# Advanced NO<sub>x</sub> Sensors for Mechatronic Applications

Angela Elia<sup>1</sup>, Cinzia Di Franco<sup>1</sup>, Adeel Afzal<sup>2</sup>,  
Nicola Cioffi<sup>2</sup> and Luisa Torsi<sup>2</sup>

<sup>1</sup>CNR-IFN U.O.S. Bari, Bari,

<sup>2</sup>Department of Chemistry, University of Bari, Bari,  
Italy

## 1. Introduction

Vehicle emissions represent an increasing contributor to air pollution in urban and country areas which gives rise to a range of environmental problems related to air quality. This has led to increasingly stringent regulatory laws on exhaust emissions level and composition.

The US regulations, signed in Dec. 2000, set new standards for measurement of automotive exhaust emissions. The emission limits for regulated species, such as carbon oxides (CO and CO<sub>2</sub>), hydrocarbons (THC), and nitrogen oxides, i.e. NO, NO<sub>2</sub>, N<sub>2</sub>O (referred as NO<sub>x</sub>), are being reduced, and new components such as methanol and formaldehyde are being added to the list of monitored species. In Japan, diesel emission standards require that in-use on-road light commercial vehicles should meet NO<sub>x</sub> emission of 0.25 g/km starting from the end of 2005 and achieve full implementation by 2011 (Nakamura et al., 2006). The European Commission has also introduced a series of regulations, the so called EURO Emission directives, from Euro I in 1991 to tighter limitations in 2009 (Euro V 80 g/km) and 2014 (Euro VI 0.08 g/Km), to meet the air quality standards stated by the international agencies (van Asselt & Biermann, 2007). The standard and validated on-line technologies for regulated emissions are effective at monitoring few components, but are limited in their use for measuring other gases. Single-wavelength non-dispersive infrared filters for CO and CO<sub>2</sub> monitoring cannot be used for other species due to interferences from water and other molecules. Chemiluminescence analyzers, which traditionally are used to measure NO<sub>x</sub> compounds, cannot differentiate NO from NO<sub>2</sub> in the same test, nor identify the other NO<sub>x</sub> gases. Flame ionization detectors cannot differentiate individual hydrocarbons. To measure raw exhaust, each technique requires a cold trap for water vapour, which can affect the concentrations of other gases. In addition, calibrations are necessary for each analysis, avoiding on-line and real-time emission monitoring.

To sample other gases in the exhaust, bag samples must be collected and taken to a laboratory for further analysis. Expensive dilution equipment must be used to prevent water condensation in the bag. Each bag sample gathers exhaust for several minutes, therefore the final result of the test is an integrated average of the gas concentrations and all time resolution is lost. Methanol and formaldehyde samples are collected with impingers, which dissolve the gases by passing them through a water-based solution. The extract is then analyzed using high-performance liquid chromatography (HPLC). Gas chromatography

(GC) can measure many of the other hydrocarbons in a bag sample with high resolution and accuracy. While HPLC and GC are effective and widely used, they are unable to track transient concentration information.

The ideal analyzer for emissions testing would combine the advantages of on-line, real-time analysis with the accuracy and speciation of laboratory-based methods. Changes in emissions chemistry that occur with changes in engine speed and torque need to be measured every second. The analyzer must be able to identify the point at which exhaust levels are reduced by the catalyst as it heats up.

New emissions regulations are forcing auto, diesel and catalyst producers to better understand combustion and emission reduction processes. The optimization of these processes requires sub-second analytical data and new methodologies to monitor gas species such as  $\text{NH}_3$  and  $\text{N}_2\text{O}$  that are not currently monitored by traditional analyzers.

Among the different pollutants present in vehicle exhaust, nitric oxide (NO) detection is of particular interest. NO is emitted from the exhausts of both gasoline and diesel engine vehicles and is generated during high temperature combustion processes from the oxidation of nitrogen in the air or fuel. NO contributes to ground-level ozone (Alving et al., 1993), acid rains and a variety of adverse human health effects (Seinfeld & Pandis, 1998), which have led to increasingly stringent regulatory mandates on the emission of NO.

Thus, accurate and reliable real-time NO sensors are required as an important part of any control system. In particular, the measurement of NO directly in the engine or in the exhaust could link into engine management systems for its control and its in situ measurement could also be used to test the catalytic converter efficiency. Over the years, a huge number of optical and electronic technologies have been developed and applied to produce sensors with remarkable sensitivity toward nitric oxide and efficient response (and recovery) kinetics. In this chapter, particular emphasis will be given on the recent achievements and ground-breaking results obtained in the past few years, namely 2008-2011, in the field of both optical and electronic  $\text{NO}_x$  sensors.

$\text{NO}_x$  optical sensor technology is among the fastest growing for mechatronic applications, as a result of its high sensitivity and selectivity, high speed, accuracy, and capability of multi-species detection. On the other hand, they need sophisticated and cumbersome equipments. In this chapter, novel spectroscopic sensing schemes suitable for the integration in high performance automated inspection systems will be reviewed.

Electronic metal oxide devices offer the advantages of low cost, low cross sensitivity to humidity and an output signal which is easy to be read and processed. Disadvantages, however, include limitations for operating at high temperatures, signal drift over time, limited selectivity or sensitivity as well as high power consumption. For these reasons, the use of novel materials such as innovative nanostructures, in place of metal-oxides, is being widely investigated in chemiresistors and transistor based device structures. Improvements have been seen for selectivity, but operation at high temperature is still an open issue.

## 2. Mid infrared absorption spectroscopy

Optical absorption methods represent a valid alternative to traditional extractive methods having the potential for fast, sensitive, accurate, selective and in situ measurements even in the presence of harsh conditions in terms of temperature, pressure, gas composition and presence of particulate.

Different spectroscopic schemes, based on the absorption of electromagnetic radiation by the gas sample, have been developed. The empirical relationship relating the absorption of

light to the composition of the gas mixture, when the light travels through, is given by the Lambert-Beer law. In the absence of optical saturation and particulate-related scattering, the absorbance is proportional to the concentration of gas. So, the gas concentration can be obtained from the absorption spectrum with a predetermined correlation.

Mid-infrared spectroscopic schemes show particular promise owing to the potential for accessing strong infrared (IR) absorption transitions. In the mid-infrared region of the electromagnetic spectrum 2.5 - 25  $\mu\text{m}$  (fingerprint region), most molecular species exhibit a unique spectral signature, i.e. a characteristic series of fundamental absorption lines due to transitions between rotational-vibrational states, characterized by very large cross-sections.

Engine exhaust emissions can be successfully analyzed by Fourier Transform Infrared (FTIR) and laser based spectroscopic techniques. Their advantages over more traditional measurement techniques include direct sampling of raw exhaust, measurement of many compounds with one analyzer and highly-stable calibrations.

In the following paragraphs we will report on innovative solutions for sensitive and selective NO monitoring in vehicle exhaust based on IR spectroscopic techniques.

### 2.1 Fourier transform infrared spectroscopy

FTIR spectroscopy is known as a reliable, self-validating and powerful tool for vehicle emission analysis due to its multicomponent detection capability, sensitivity and time resolution (Adachi, 2000; Durbin, 2002). It is especially well suited for monitoring non-regulated pollutants when testing alternative fuels and newer emission-control technologies. The FTIR technique is a well established methodology which has been validated by several regulatory and standardization agencies for extractive gas-sampling analysis (EPA, 1998; Reyes, 2006). Many highly reactive species in the exhaust can be simultaneously measured by FTIR even below part-per-million levels, replacing several discrete analyzers which may require complicated calibration procedures.

The analyzer developed by the Thermo Fischer Scientific Company, Antaris IGS, allows concentrations of up to 40 gases to be calculated simultaneously at one-second intervals (Thermo, 2007) and requires minimal maintenance and recalibration.

The MultiGas™ 2030 HS by MKS Instruments (Tingvall et al., 2007), has been designed to measure both traditional and non-traditional combustion emissions gases. The system incorporates a patented fast scanning FTIR capable of providing high resolution ( $0.5\text{ cm}^{-1}$ ) data at 5 Hz frequency. The system was also configured to allow combustion exhaust to flow through the 200 mL gas cell at rates up to 100 L/min to prevent diffusion and measurement delay. The software and computer hardware provided with each system are optimized to allow the simultaneously quantification of 20 gases.

Reyes and co-workers developed a method to acquire valuable information on the chemical composition and evolution of emissions from typical driving cycles of a Toyota Prius hybrid vehicle in the Mexico City Metropolitan Area (Reyes, 2006). The analysis of the gases is performed by passing a constant flow of a sample gas from the tail-pipe into a 10 L multi-pass cell. The absorption spectra within the cell are obtained using an FTIR spectrometer at  $0.5\text{ cm}^{-1}$  resolution along a 13.1 m optical path. Additionally, the total flow from the exhaust is continuously measured from a differential pressure sensor on a Pitot tube installed at the exit of the exhaust. This configuration aims to obtain a good speciation capability by co-adding spectra during 30 s and reporting the emission of NO and other non-regulated pollutants.

## 2.2 Quantum cascade laser-based optical techniques

The development of mid infrared detection laser-based techniques has received a significant boost from the invention and optimization of efficient mid-infrared semiconductor laser sources which can effectively substitute optical methods based on the study of overtones and combination of lines, falling in the near-infrared spectral region, where the absorption cross sections drop by orders of magnitudes.

Among the absorption techniques, direct absorption spectroscopy, cavity enhancement approaches and photoacoustic (PA) spectroscopy have the potentiality to give sensitive and selective sensors for on-line and in-situ applications. The first two techniques take advantage of long optical path length absorption in multi-pass cells and high finesse optical cavities, respectively. Although they are characterized by high sensitivity, they need sophisticated and cumbersome equipments. More compact and transportable sensors can be obtained by using the photoacoustic spectroscopy, which presents many advantages, i.e. high sensitivity (up to parts per billion detection limits), compact set-up, fast time response and portability.

In the mid infrared region traditional source options include gas lasers (CO, CO<sub>2</sub>), lead-salt diode lasers, coherent sources based on difference frequency generation (DFG) and optical parametric oscillators (OPOs). While these lasers have allowed effective spectrometers with trace-level sensitivity, they have several disadvantages: lack of continuous wavelength tunability and large size and weight of gas lasers, low output power and cooling requirement of lead salt diode lasers, inherently low infrared power and finite line width of nonlinear optical devices.

The development of innovative mid infrared laser sources, the quantum cascade lasers (QCLs), has given a new impulse to infrared laser-based trace gas sensors. QCLs are unipolar semiconductor lasers based on intersubband transitions in a multiple quantum-well heterostructure. They are designed by means of band-structure engineering and grown by molecular beam epitaxy techniques (Faist et al., 1994).

The benefit of this approach is a widely variable transition energy primarily regulated by the thicknesses of the quantum well and barrier layers of the active region rather than the band gap as in diode lasers. Typical emission wavelengths can be varied in the mid-infrared range 3.5–24  $\mu\text{m}$  up to THz. Moreover, they are characterized by single-frequency operation, narrow linewidth (< 30 MHz), high powers (up to few watts), and continuous wave (cw) operation also at room temperature.

To date, QCLs have been used for measurements of different gases (NO, CO<sub>2</sub>, NH<sub>3</sub> etc.) in industrial and vehicle exhaust emission with sensitivities in the range of the parts per million/trillion by volume (ppmv/ppbv) (Kosterev & Tittel, 2002a; Elia et al., 2011).

In the following sections, innovative quantum cascade laser-based optical sensors for NO detection, in automotive exhaust applications, will be reviewed.

### 2.2.1 Direct absorption spectroscopy

Direct absorption spectroscopy based on quantum cascade laser has been extensively studied in the last years for in situ measurements of gas components in vehicle exhaust (Weber et al., 2002; McCulloch et al., 2005; Kasyutich et al., 2009; Hara et al., 2009).

QCL-based absorption analysers offer an improvement in performance, higher sensitivity and selectivity, even at low concentrations, with respect to the other spectroscopic schemes.

Kasyutich et al. (Kasyutich et al., 2009) measured NO in the direct exhaust gas of a gasoline engine, whose operating conditions can be varied in a controlled manner, with a sensitivity

of 8 ppmv. They measured NO concentrations in real-time in the range 0 - 2000 ppmv with a temporal resolution (1 s) suitable to respond to changes in engine operating conditions. Figure 1 reports the main components of the mid-IR spectrometer based on a thermoelectrically-cooled cw single mode quantum cascade laser used for NO measurements in the exhaust of a static internal combustion engine.

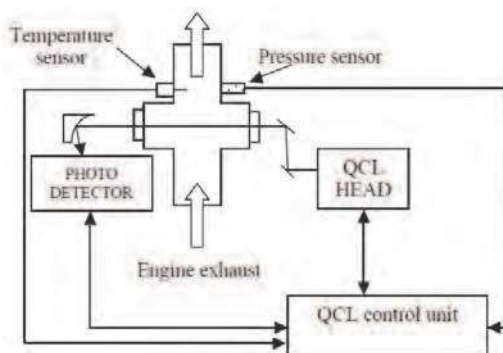


Fig. 1. Experimental setup for NO measurements on engine exhaust (reproduced with permission from Kasyutich et al., 2009. IOP Publishing).

The radiation emission of the single mode QCL was tuned over the strong NO absorption doublets  $R(6.5)$  at 1900.075 (free of interference from strong water absorption lines) by applying a modulation voltage waveform. Concentrations were determined in real-time by a non-linear least-squares fitting routine by measuring the attenuation of the beam due to the light absorption by NO molecules. A minimum detectable optical depth of 0.0018 was estimated at signal to noise ratio (SNR) of 1 corresponding to a NO detection limit of 8 ppmv. The engine used in the tests was a Rover K series version. The mid-infrared QCL beam probed the 2-inch diameter stainless steel exhaust pipe 2.5 m away from the engine. The temperature and pressure of the exhaust gas were monitored just above the measurement point as reported in the figure. To allow optical access to the exhaust pipe, a cross-piece was inserted with two wedged sapphire windows mounted 23 cm apart.

In 2010 Horiba (Horiba, 2010) presented a new emission measurement system for NO, NO<sub>2</sub>, N<sub>2</sub>O and NH<sub>3</sub> gases (MEXA-1400QL-NX). Sample gas is fed into the gas cell and a laser pulse irradiates into the gas cell. The laser radiation emitted as continuous pulse is detected after a multiple reflection between two mirrors in the gas cell. From its inherent design and control, the wavelength of QCL radiation slightly varies with temperature therefore it is possible to scan the constant width of the wavelength in a particular region. Figure 2 shows the block diagram of the HORIBA QCL-based analyzer. Four laser elements corresponding to one measurement component respectively (NO, NO<sub>2</sub>, N<sub>2</sub>O and NH<sub>3</sub>) are used in the device. The wavelengths of the respective laser elements are selected and controlled in order to have emission in a region where a spectrum peak falls with negligible interference from other environmental gases, such as CO, CO<sub>2</sub>, H<sub>2</sub>O. The analyzer design has two paths in a single sample cell; the short path with only few light reflections and the long path with multiple light reflections. The combination of two path lengths allows measuring both high concentration and low concentration gases providing a wide dynamic range measurement.

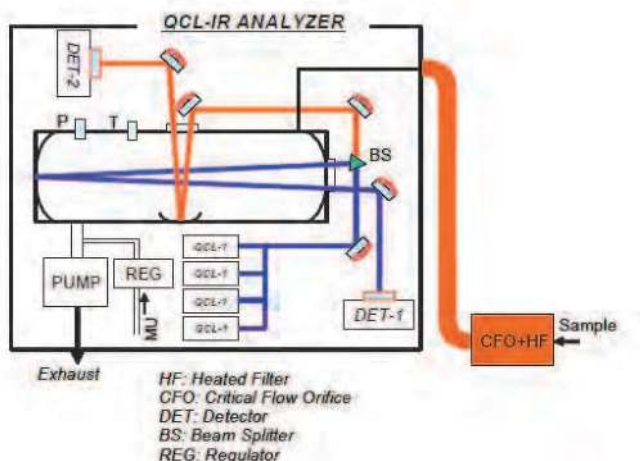


Fig. 2. Experimental setup of HORIBA QCL-based analyzer (reproduced with permission from HORIBA).

In comparison with FTIR systems, the results of measurements made using QCL technology are significantly more precise at low concentrations and offer a wider dynamic range of measurement. The finer resolution of the absorption spectrum makes QCL-based NO sensors less sensitive to incidental interference from other gases such as CO, CO<sub>2</sub>, CH<sub>4</sub>, H<sub>2</sub>O and THC. In addition to the higher sensitivity and selectivity, these sensors also do not suffer from the interference of NO<sub>x</sub> measurement by NH<sub>3</sub> typical of the chemoluminescence analysers.

### 2.2.2 Cavity ringdown spectroscopy

Cavity ringdown spectroscopy (CRDS), first demonstrated by O'Keefe and Deacon (O'Keefe & Deacon, 1988) in 1988, is one of the cavity enhanced spectroscopy methods which provides a much higher sensitivity than conventional long optical path length absorption spectroscopy due to its ability to achieve a long optical path in a compact sampling cell.

Sumizawa et al. reported the accurate and precise measurement of nitric oxide in automotive exhaust gas using a thermoelectrically cooled, pulsed quantum cascade laser as a light source and cavity ring-down spectroscopy (Sumizawa et al., 2010).

This technique, which can be performed with pulsed or continuous light sources, is based on the measurement of the decay time of an injected laser beam in a high-finesse optical cavity in the presence of an absorbing gas by measuring the time dependence of the light leaking out of the cavity. In particular, in the case of pulsed lasers, a short laser pulse is injected into a high finesse optical cavity to produce a sequence of pulses leaking out through the end mirror from consecutive traversals of the cavity by the pulse. Typically, the laser pulse is short and has a small coherence length compared to a relatively large physical cavity length. Under these conditions interference effects are avoided and the intensity of the cavity pulses decays exponentially with a time constant (ringdown time) defined by:

$$\tau = \frac{l}{c} \frac{1}{\alpha l + (1 - R)}$$

Where  $l$  is the cavity length,  $c$  is the speed of light,  $R$  is the reflectivity of the cavity mirrors ( $R \approx 1$ ) and  $\alpha$  is the absorption coefficient of the sample filling the cavity. Thus, the absorption coefficient can be determined by measuring the decay rate without ( $\tau_{empty}$ ) and with ( $\tau$ ) the absorbing gas present with the following equation:

$$\alpha = \frac{1}{c} \left( \frac{1}{\tau} - \frac{1}{\tau_{empty}} \right)$$

In Figure 3, the schematic of the CRDS-based NO sensor developed by Sumizawa and co-workers is reported. To detect fundamental vibrational transitions of NO, they used a pulsed QCL operated near 5.26  $\mu\text{m}$ . The output of the QCL is focused with a lens ( $L_1$ ) on the center of the high finesse optical cell. At both ends of the stainless steel cell (500 mm long) two high-reflectivity ZnSe mirrors with a 25.4 mm diameter and a 1 m radius of curvature are mounted. A lens ( $L_2$ ) was placed after the cell to collect the transmitted light on an amplified liquid nitrogen-cooled InSb detector. The ringdown decay curves were measured and then stored on a computer memory.

The vehicle used for real time NO monitoring in exhaust gas was a light duty truck with a 4.8 L diesel engine equipped with a common rail injection system and a diesel oxidation catalyst. The analyzed sample gas was made by diluting the exhaust gas with ambient air filtered by HEPA and charcoal filters using a constant volume sampler. The diluted exhaust gas was introduced into the cell at a constant flow; a membrane gas dryer was used to avoid interference by water. An HEPA filter was introduced to eliminate particles  $> 0.3 \mu\text{m}$  in diameter which would lead to arbitrary loss of light in the cell.

The sensor demonstrated a minimum detection limit of NO  $\approx 50$  ppbv in a 20 s averaging time for a signal-to-noise ratio of 2.

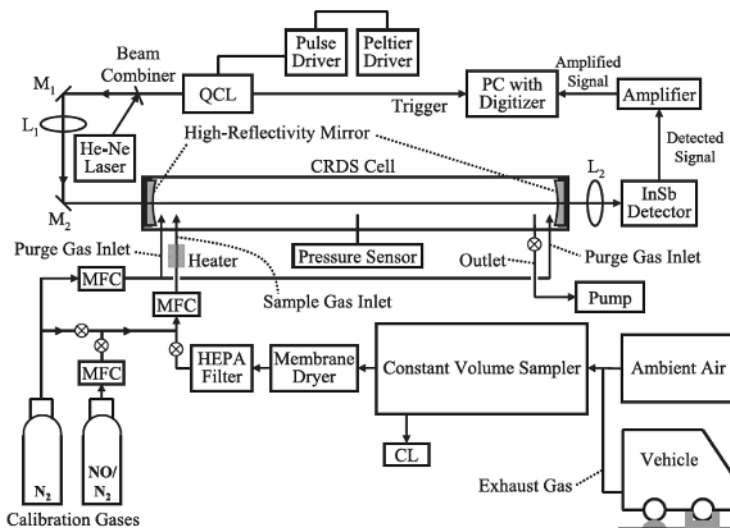


Fig. 3. Experimental setup of CRDS-based exhaust-gas NO sensor (reproduced with kind permission from Sumizawa et al., 2010. Springer Science+Business Media).

The NO exhaust measurement obtained from the CRDS-based NO sensor in a vehicle test run under the JE05 cold start cycle was in agreement with the simultaneous results from a conventional chemiluminescence NO<sub>x</sub> sensor. Stable measurement in diluted exhaust gas sample with a concentration from sub-ppmv to 100 ppmv for more than 30 minutes and with a time resolution of 1 s was demonstrated.

### 2.2.3 Quartz enhanced photoacoustic spectroscopy

An effective method for sensitive trace gas detection in mechatronic applications is photoacoustic spectroscopy coupled with QCLs. PAS is an indirect technique in which the effect on the absorbing medium and not the direct light attenuation is detected. It is based on the photoacoustic effect, i.e. the generation of a pressure wave resulting from the absorption of modulated light of appropriate wavelength by gas molecules. The amplitude of this wave is directly proportional to the gas concentration and can be detected via a resonant transducer. Traditionally, the pressure wave is detected via one or more microphones (Elia et al., 2005; Di Franco et al., 2009; Elia et al. 2009). In 2002 (Kosterev et al., 2002b), an innovative method, the Quartz Enhanced Photoacoustic Spectroscopy (QEPAS), has been proposed by Kosterev et al.

The key issue of QEPAS is the detection of optically generated pressure wave via a rugged sharply resonant piezoelectric transducer, a quartz tuning fork (QTF), with a resonant frequency close to 32,768 (i.e., 2<sup>15</sup>) Hz (Kosterev et al., 2002b; Kosterev et al., 2005) The mode at this frequency corresponds to a symmetric vibration. A mechanical deformation of the QTF prongs caused electrical charges on its electrodes. The resulting system exhibits unique properties such as an extremely high quality factor (Q-factor) of > 10,000, small size, immunity to environmental acoustic noise and a large dynamic range.

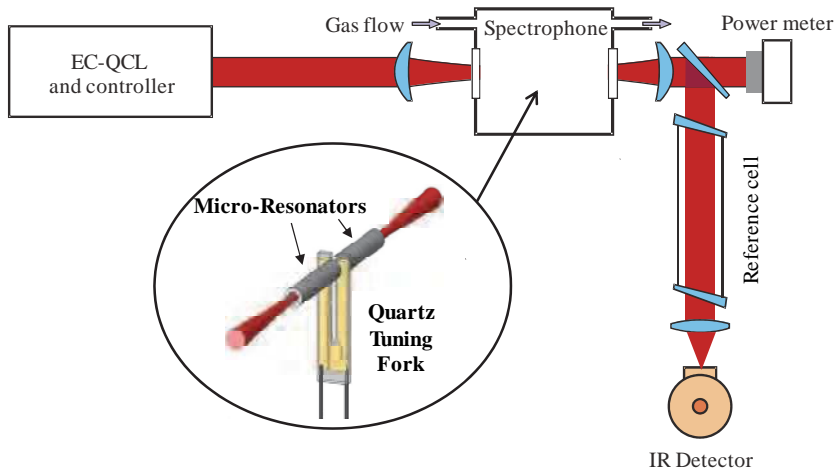


Fig. 4. Schematic of EC-QCL based QEPAS sensor.

In figure 4 typical QEPAS-based sensor configuration is reported. The module to detect laser-induced pressure wave is a spectrophone which consists of a QTF and a microresonator. It is made of a pair of thin tubes and increases the effective interaction length between the radiation-generated pressure wave and the QTF. The tubes are aligned



perpendicular to the QTF plane. The distance between the free ends of the tubes is equal to half wavelength of sound in air at 32.75 kHz, thus satisfying the resonant condition. Experiments have shown that the microresonator yields a signal gain of 10 up to 20.

Spagnolo and co-workers reported the development and performances evaluation of a QEPAS based NO sensor, utilizing a cw, thermoelectrically cooled, external cavity quantum cascade laser (EC-QCL) as a light source operating at 5.26  $\mu\text{m}$  (Spagnolo et al., 2010). The EC-QCL allows to access the strong and quasi interference-free NO absorption doublet R(6.5) at 1900.075  $\text{cm}^{-1}$ . They performed a wavelength modulation technique by sinusoidally modulating the injection current of the laser at half of the QTF resonance frequency ( $f=f_0/2\sim 16.20$  kHz), while slowly scanning the laser wavelength. The corresponding photoacoustic spectra were obtained by demodulating the detected signal at the frequency  $f_0$  using a lock-in-amplifier.

The NO detection in automotive exhaust assumes the presence of water vapor in the gas sample. Therefore, it is important to study the H<sub>2</sub>O influence on the NO sensor performance. The V-T (vibration-to-translation) energy transfer time  $\tau_{VT}$  for NO is dependent on the presence of other molecules and intermolecular interactions. The QEPAS measurements that are performed at a detection frequency 32 kHz are more sensitive to the vibrational relaxation rate compared to the conventional PAS which is commonly performed at < 4 kHz frequency  $f$ . In case of slow V-T relaxation with respect to the modulation frequency ( $\omega\tau_{VT}\gg 1$ , where  $\omega=2\pi f$ ), the translational gas temperature cannot follow fast changes of the laser induced molecular vibrational excitation. Thus, the generated photoacoustic wave is weaker than it would be in case of instantaneous V-T energy equilibration. Due to the high energy of first vibrational state of NO, the V-T energy transfer is slow, e.g. in dry N<sub>2</sub> the relaxation time is  $\tau_{VT} = 0.3$  ms and so  $\omega\tau_{VT}\gg 1$ . The addition of H<sub>2</sub>O vapor enhances the V-T energy transfer rate and, thus, the detected QEPAS signal amplitude. Once the  $\omega\tau_{VT}< 1$  condition is satisfied, the amplitude of the PA signal is not affected by changes of  $\tau_{VT}$ .

In this signal saturation condition, authors demonstrated a NO concentration resulting in a noise-equivalent signal of 15 ppbv. The higher sensor performances, the compactness, and the role of water (generally interfering specie for other sensors) make QEPAS a promise in commercial sensors for automotive applications.

### 3. Electronic sensors

Electronic sensors are commonly produced by fabricating metal- or metal oxide-based nanostructured materials, which may provide long-term, reproducible and selective gas sensing performance. In fact, it is well-known that absorption or desorption of gas molecules on the surface of a metal oxide changes the conductivity (or resistivity) of the material, a phenomenon - first revealed by (Seiyama et al., 1962) using zinc oxide (ZnO) thin film layers. Since then, electronic (semiconductor) sensing has come a long way thanks to a huge flux of research in this field resulting into the achievement of sensitivities of electronic sensors to the order of parts per billion (ppb) toward various gases such as NO<sub>x</sub> (Gurlo et al., 1998; Guo et al., 2006; Kida et al., 2009). In addition, advances in fabrication technology enabled the production of low-cost sensors with improved sensitivity and reliability compared to those formed using conventional methods (Williams, 1999). Subsequent paragraphs give a brief introduction to the mechanism of electronic detection, and structure of the sensing elements and their types.

### 3.1 Principle of electronic sensors

According to band theory (Hoch, 1992), within a crystal lattice there exists a valence band and a conduction band, separated from each other as a function of energy (band gap), particularly the Fermi level that is defined as the highest available electron energy levels at a  $T = 0$  K. Generally semiconductors have a sufficiently large energy gap i.e. in the range of 0.5-5.0 eV. Hence at energies below the Fermi level, conduction is not observed; while above it, electrons start occupying the conduction band, consequently enhancing the conductivity of a semiconductor. Over the years, band theory of solids attracted intense research with reference to semiconductor gas sensors (Yamazoe et al., 1979; Barsan et al., 1999). When gases like  $\text{NO}_x$  interact with the surface of an active layer i.e. generally through surface-adsorbed oxygen ions; it results in a change in the concentration of charge carriers of the active material. Such a change in charge carrier concentration transforms the conductivity (or resistivity) of the active layer. In an n-type semiconductor, majority of charge carriers are electrons, while a p-type semiconductor conducts with positive holes being the mainstream charge carriers. And being strongly oxidizing gases, the oxides of nitrogen ( $\text{NO}_x$ ) serve to deplete the sensing layer of charge carrying electrons, thus resulting in a decrease in conductivity of the n-type semiconductor. Conversely, in a p-type semiconductor the opposite effects are observed with the sensing material i.e. showing an increase in the conductivity.

Wei and coworkers (Wei et al., 2004) postulated the sensing mechanism of different types of tin oxide ( $\text{SnO}_x$ ) and single-walled carbon nanotube (SWCNT) composites. High sensitivity for the said nanocomposites was attributed to the expansion of depletion region on the surface of the  $\text{SnO}_2$  particles and the p-n junction between n-type  $\text{SnO}_2$  and p-type SWCNTs, when target gas molecules are adsorbed on the surface. However, in a recent work (Hoa et al., 2009a) on similar nanocomposite system, authors propose that owing to the different morphology, the characteristic response of the composite originates from the  $\text{SnO}_x$  nano-beads aligned together on the surface of SWCNTs. When these nano-beads are exposed to air/ $\text{NO}_x$ , the adsorbed  $\text{O}_2/\text{NO}_x$  molecules extract electrons out of the  $\text{SnO}_x$  beads, leading to the formation of an electron depletion layer, as shown in Figure 5.

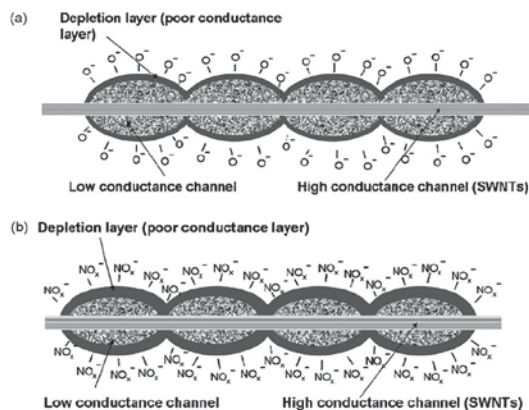
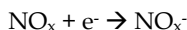


Fig. 5. The sensing mechanism model of tin oxide and SWCNTs nanocomposites based gas sensor. The surface state of nanowires structured tin oxide and SWCNTs nanocomposites in (a) air, and (b)  $\text{NO}_x$ , respectively (reproduced with permission from Hoa et al., 2009a. Elsevier).

The adsorption of NO<sub>x</sub> on the surface of SnO<sub>x</sub> can be simplified as;



Particularly, when NO<sub>x</sub> gas molecules adsorb on the surface of active layer, they capture electrons out of an n-type SnO<sub>x</sub> material (just like O<sub>2</sub> does), thus forming a depletion region. NO<sub>x</sub> adsorption, however, increases the depth of depletion region owing to the higher electron affinity (2.28 eV) of NO<sub>x</sub> as compared to the pre-adsorbed O<sub>2</sub> (0.43 eV) (Broqvist et al., 2004). Consequently, the resistance of the nanocomposite material increases and is measured as the electrical sensor response.

### 3.2 Device structure and types

Electronic sensors are usually based on Metal Insulator Semiconductor Field Effect Transistors (MISFET), and utilize metal and/or metal oxide nanostructured material as the catalytically active sensing layers. The field effect devices are sub-divided into different categories; transistors, Schottky diodes or capacitors, with transistors being the preferred choice for commercial applications (Mandelis and Christofides, 1993). Figure 6 presents an overview of the different types of devices.

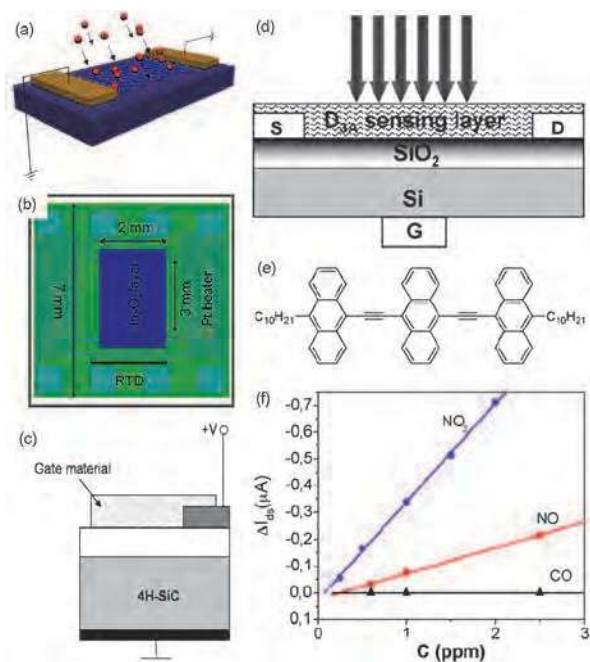


Fig. 6. The schematic diagrams of (a) graphene-based NO<sub>2</sub> gas sensor; (b) In<sub>2</sub>O<sub>3</sub>-based NO<sub>x</sub> sensor with inter-digitated electrodes; and (c) MIS field effect capacitive sensor. (d) A bottom gate organic thin film transistor (OTFT); (e) a novel organic semiconductor (D3A) used as the OTFT's active layer; and (f) its selective response to various gases at room temperature (adapted with permission from Ko et al., 2011; Kannan et al., 2010a; Marinelli et al., 2009. Elsevier).

A schematic diagram of the simplest electronic sensing device, a chemiresistor, is shown in Figure 6a. Ko et al (Ko et al., 2011) employed a graphene-based NO<sub>2</sub> gas sensor to study absorption/desorption of gas molecules on the surface of graphene. The device is fabricated by depositing graphene layers via standard scotch tape method (Novoselov et al., 2004) on a pre-defined SiO<sub>2</sub>/Si substrate. The electron-beam lithography is used to form two metal contacts on to the graphene layer, followed by electron-beam evaporation of Pd/Au. The device is then used to obtain the current-voltage characteristics of graphene-based gas detectors at various concentrations of NO<sub>2</sub> gas.

Kannan and coworkers (Kannan et al., 2010a; 2010b) also fabricated NO<sub>x</sub> sensors using a micro hotplate die, and a 0.3mm thick, 76.2mm Si wafer with 400nm thermally grown SiO<sub>2</sub> (Figure 6b). The resistance heater and inter-digitated Pt electrodes (IDE) are fabricated using a lift off process. They employed four distinct dies with varying IDE spacing. In<sub>2</sub>O<sub>3</sub> based active films of controlled thickness are RF sputter deposited. These devices are subsequently tested for NO<sub>x</sub> response discussed later in this chapter.

Figure 6c shows a typical field effect MIS (Metal-Insulator-Semiconductor) capacitor with a gate electrode. The capacitive sensor consists of p-doped Si as semiconductor, with a thermally grown oxide as insulator. The ohmic backside contact comprised of evaporated, annealed Al; while Cr/Au bonding pads are evaporated on top. The device is covered by a layer of catalytically active Au-NPs, and then mounted on a 16-pin holder along with a ceramic heater and a Pt-100 element to perform gas sensing measurements (Ieva et al., 2008; Cioffi et al., 2011).

In Figure 6d the structure of an organic thin film transistor (OTFT) is reported (Marinelli et al., 2009). It is a bottom gate OTFT with the organic semiconductor acting both as transistor channel and as sensing layer. Figure 6e shows the chemical structure of the 9, 10-bis[(10-decylnanthracen-9-yl)ethynyl]anthracene molecule (D3A). The D3A is deposited as sensing layer via spin coating onto a SiO<sub>2</sub> (100nm)/n-doped Si substrate, where Au/Ti source (S) and drain (D) pads were photo-lithographically patterned. Authors reported that when the D3A OTFT was exposed to different gases like NO<sub>2</sub>, NO and CO, concentrations as low as 250 ppb of NO<sub>2</sub> could be detected. The response-concentration regression lines for NO, CO and NO<sub>2</sub> are reported in Figure 6f, which shows that D3A OTFT sensor has very low cross sensitivities toward interfering gases and that linear dependency of sensor response on concentration is observed.

### 3.3 Active nanomaterials and sensor performance

A few exemplary electronic sensors, for instance, those based on graphene, indium oxide, gold nanoparticle, and organic semiconductor, have been discussed so far. To date, several other NO<sub>x</sub> sensors have been proposed and examples of such devices include: semiconducting metal oxide sensors (GuO et al., 2008; Hwang et al., 2008; Wang et al., 2008; Hoa et al., 2009a; Navale et al., 2009, Qin et al., 2010; Firoz et al., 2010) and resistive sensors based on metal-phthalocyanines (Oprea et al., 2007; Shu et al., 2010 ), conjugated systems (Naso et al., 2003; Nomani et al., 2010) as well as carbon nanotubes (Sayago et al., 2008; Ueda et al., 2008) and nanocomposites (Balazsi et al., 2008; Kong et al., 2008; Hoa et al., 2009b; 2009c; Leghrib et al., 2010). The scientific research community is currently focusing on the development and investigation of novel materials, which are sensitive toward NO<sub>x</sub> gases as well as appropriate and well-suited for the solid-state gas sensors. The most promising semiconductor materials for the fabrication of NO<sub>x</sub> sensors are noble metals such as Gold

(Au) and metal oxides such as SnO<sub>2</sub>, WO<sub>3</sub>, In<sub>2</sub>O<sub>3</sub>, and ZnO nanostructures; since they afford high surface area for active layer-gas interaction, and satisfactory selectivity.

To adsorb as much of the target gas as possible on the surface, it is desirable that these active layers have a large surface area so as to give a stronger and easily measurable electrical signal e.g. to trace amounts of NO<sub>x</sub>; and this has been accomplished by manipulating active materials into nano-regime. Manipulating and controlling sensing events at the molecular scale simultaneously avoids several problems associated with traditional sensor technologies. Incidentally, nanotechnology offers unique advantages to the sensor industry in terms of sensitivity, and rapid response and recovery kinetics due to larger surface-to-bulk ratio. An important feature of these nanomaterials, in addition, is the possibility to tailor the properties by varying the size and morphology of nanostructures, which in turn affects the electrical properties of materials.

Ahn et al (Ahn et al., 2009) fabricated ZnO nanowires on-chip via selective growth of nanowires on patterned gold catalysts thus forming nanowire air bridges (nano-bridges) between two Pt electrodes, as shown in Figure 7a. These nanowires were prepared by the carbo-thermal reduction process using a mixture of ZnO and graphite powders. Figures 7b and 7d shows side- and top-view scanning electron microscope (SEM) images of well-prepared ZnO nanowires grown on patterned electrodes. Researchers found that ZnO nanowires grow only on the patterned electrodes and many nanowire/nanowire junctions exist there, which act as electrical conducting path for electrons, as shown in Figure 7c.

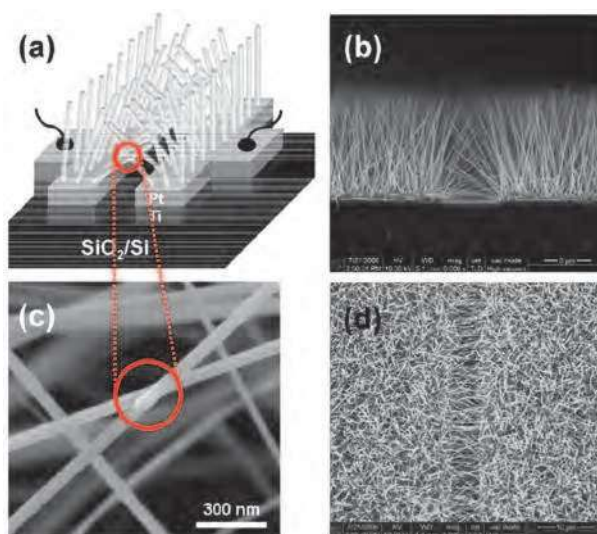


Fig. 7. (a) The schematic illustration of ZnO-nanowire air bridges over the SiO<sub>2</sub>/Si substrate. (b) Side-view and, (d) top-view SEM images clearly show selective growth of ZnO nanowires on Ti/Pt electrode. (c) The junction between ZnO nanowires grown on both electrodes (reproduced with permission from Ahn et al., 2009. Elsevier).

ZnO-based nanomaterials have rather good stability and sensing characteristics toward NO<sub>x</sub> gases combined with sufficient selectivity; that is why they have been studied widely in the past two years. Carotta et al (Carotta et al., 2009), for instance, compared ZnO nanoparticle-

and nanotetrapod-based thick film  $\text{NO}_x$  sensors. Oh and coworkers (Oh et al., 2009) fabricated a high-performance  $\text{NO}_2$  gas sensor based on vertically aligned ZnO nanorod arrays grown via ultrasonic irradiation. Shouli et al (Shouli et al., 2010) studied different morphologies of ZnO nanorods and their sensing properties towards  $\text{NO}_2$ . These nanorods were grown via hydrothermal and sol-gel processes using different surfactants.

Zhang et al (Zhang et al., 2009) produced  $\text{SnO}_2$  hollow spheres mediated by carbon microspheres. Authors report that carbon microspheres derived from hydrothermal conditions are hydrophilic with plenty of  $-\text{OH}$  and  $\text{CO}$  groups on the surface, which enable them to bind metal cations. Such carbon microspheres loaded metal cations give rise to hollow metal oxide spheres after calcination at high temperatures. Transmission electron microscopy (TEM) images of  $\text{SnO}_2$  hollow spheres calcined at  $450^\circ\text{C}$  are shown in Figure 8a. Researchers demonstrated that the hollow spheres have a rough morphology with a diameter in the range of 500–700 nm. Shell details are clearly visible in Figures 8b–8d, which reveal that the porous shells are formed with a thickness of about 25 nm. Figure 8e shows the diffraction rings in the selected-area electron diffraction (SAED) pattern verifying the polycrystalline structure of  $\text{SnO}_2$  hollow spheres. These hollow sphere  $\text{NO}_2$  gas sensors present excellent selectivity and relatively swift response kinetics.

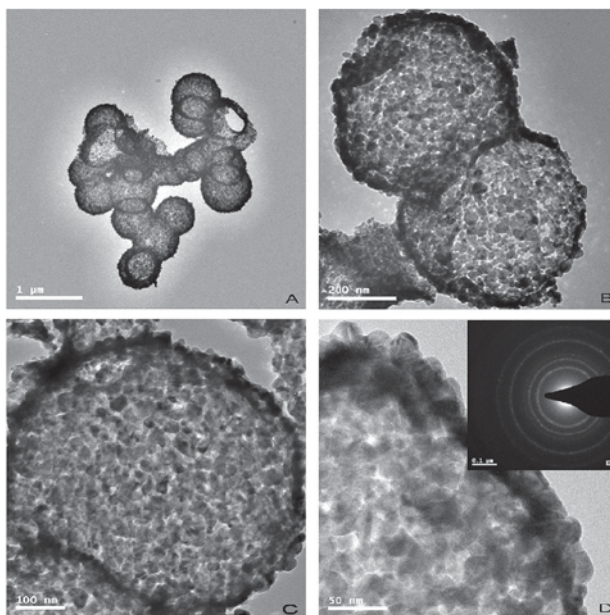


Fig. 8. (a–d) TEM images and (e) SAED pattern of  $\text{SnO}_2$  hollow spheres calcined at  $450^\circ\text{C}$  (reproduced with permission from Zhang et al., 2009. Elsevier).

Zhang and coworkers (Zhang et al., 2010) fabricated atmospheric plasma-sprayed  $\text{WO}_3$  coatings for sub-ppm (i.e. 0–450 ppb) level  $\text{NO}_2$  detection. Park et al (Park et al., 2010) employed  $\text{SnO}_2$ -ZnO hybrid nanofibers as active layers for  $\text{NO}_2$  sensing via combining electro-spinning and pulsed laser deposition methods. These nanofibers exhibited high response to  $\text{NO}_2$  gas concentrations as low as 400 ppb at  $200^\circ\text{C}$ .  $\text{In}_2\text{O}_3$ -ZnO composite films

(Lin et al., 2010) were also fabricated to investigate NO<sub>x</sub> gas sensing characteristics, and it was found that composite films with In/Zn ratio of 0.67 reached detection limits of 12 ppb at 150°C.

The sensor responses of the gas sensors with channels composed of the as-pasted and the heat-treated ZnO nanoparticles are plotted in Figure 9a and 9b, respectively. Jun et al (Jun et al., 2009) reported that controlled heat-treatment of the ZnO nanoparticles at 400 °C led to their necking and coarsening, which resulted in a decrease in the number of particle junctions (junction potential barrier), thus reducing resistance in the presence of ambient air. However necking of the particles had an opposite effect when interacting with NO<sub>x</sub>, as necked particles of small sizes become fully depleted due to removal of electrons, hence increasing the sensor response.

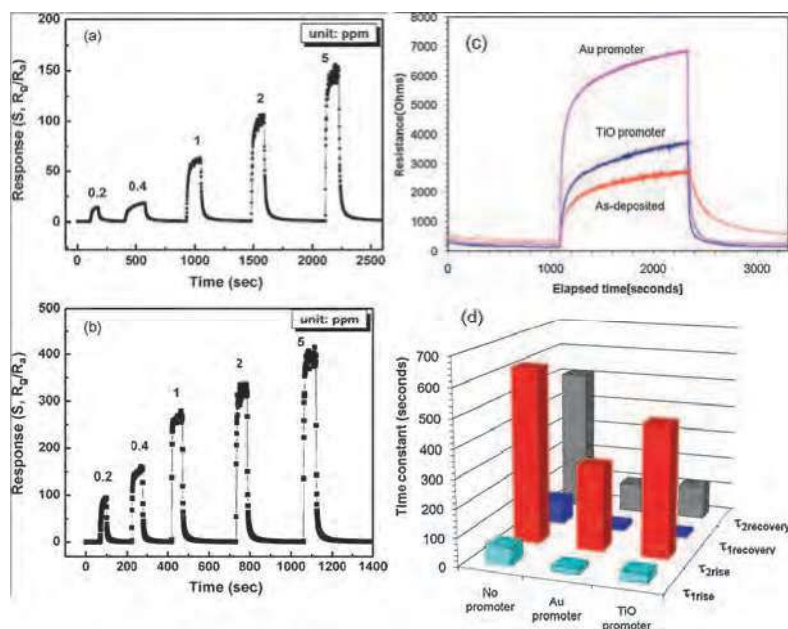


Fig. 9. Responses of the (a) as-pasted and (b) heat-treated ZnO NPs as a function of the injected NO<sub>2</sub> gas concentration at 200 °C. (c) Response of the as-deposited, TiO<sub>x</sub> promoter and Au promoter In<sub>2</sub>O<sub>3</sub> films (d) Time constants for the rise and recovery from exposure to 25ppm NO<sub>x</sub> for as-deposited, TiO<sub>x</sub> promoter and Au promoter in ambient N<sub>2</sub> at 500 °C. (adapted with permission from Jun et al., 2010; and Kannan et al., 2010a. Elsevier).

Kannan et al (Kannan et al., 2010a; 2010b) fabricated chemiresistors with inter-digitated electrode (Figure 2b) with RF sputtered In<sub>2</sub>O<sub>3</sub> thin film (150 nm) either with or without promoter layers, for instance, Au or TiO<sub>x</sub>. Promoter layers act as additives on a semiconductor support (In<sub>2</sub>O<sub>3</sub>), and help improve the sensing characteristics. Figure 9c and 9d present the sensor response of 150nm thick In<sub>2</sub>O<sub>3</sub> films as a function of the promoter layers to 25 ppm NO<sub>x</sub> in N<sub>2</sub> carrier gas operating at 500°C. In<sub>2</sub>O<sub>3</sub> film with Au-promoter layer shows the faster and highest sensor response that is largely attributed to the spillover mechanism i.e. NO<sub>x</sub> strongly adsorbs on the Au surface and spills over to the In<sub>2</sub>O<sub>3</sub> support.

Metallic nanoparticles such as gold (Au) exhibit high sensitivities toward NO<sub>x</sub> gases (Hanwell et al., 2006; Ieva et al., 2008). Cioffi and coworkers (Cioffi et al., 2011) synthesized core-shell gold nanostructure electrochemically, according to the so-called Sacrificial Anode Electrolysis (SAE). This kind of synthesis was carried out in the presence of quaternary ammonium salts dissolved in THF/acetonitrile mixture (ratio 3:1), which act both as the supporting electrolyte and as the stabilizer by forming a shell and thus giving rise to stable Au-colloidal solution. These nanoparticles were employed as gate material in field effect capacitive devices, shown in Figure 6c. TEM images of Au-NPs stabilized by different quaternary ammonium species are reported in Figure 10a-10c. It was found that Au nanoparticle sensor was able to detect 50-400 ppm NO<sub>2</sub>, shown in Figure 10d. Authors suggest that voltage increase upon exposure to NO<sub>2</sub> instigates from the charge donating behavior of nitrogen oxides leading to an increase in the charge density at the Au nanoparticle film-insulator interface and thereby increasing the charge carriers in the semiconductor layer.

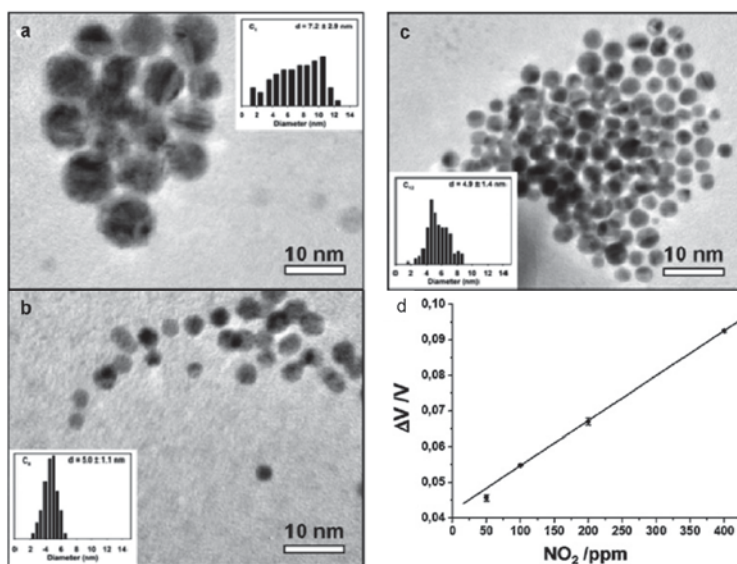


Fig. 10. TEM images and dimensional dispersion histograms (insets) of Au nanoparticles electro-synthesized in presence of (a) tetrabutyl ammonium chloride (TBOC), (b) tetraoctyl ammonium chloride (TOAC), and (c) tetradodecyl ammonium chloride (TDoAC). (d) Sensor response at operative temperature of 150°C for several NO<sub>2</sub> concentration levels in presence of an active gate layer of Au nanoparticles/TOAC (adapted with permission from Cioffi et al., 2011).

The electronic sensors based on core-shell Au-nanoparticles enable selective detection of NO<sub>x</sub> gases; and the sensitivity of such systems is influenced by the particle size. These sensors show negligible sensitivity toward interfering gases such as H<sub>2</sub>, CO, NH<sub>3</sub>, and C<sub>3</sub>H<sub>6</sub>. Although further improvement and optimization of these systems is necessary, their favored characteristics could lead them becoming ever more important tools for real-time monitoring of NO<sub>x</sub> gases.



## 4. Conclusion

Strict emission regulations and deeper environmental awareness have led to intense research into emissions reduction by engine producers and research organizations. Over the years, a huge number of optical and electronic technologies have been developed and applied to produce sensors with remarkable sensitivity toward nitric oxide and efficient response (and recovery) kinetics. In this chapter, a brief overview on the recent achievements and ground-breaking results obtained in the past few years, namely 2008-2011, in the field of both optical and electronic NO sensors have been reported.

Engine exhaust emissions have been successfully analyzed by FTIR and laser based spectroscopic techniques. Their advantages over more traditional measurement techniques include direct sampling of raw exhaust, measurement of many compounds with one analyzer and highly-stable calibrations. The FTIR technique is a validated methodology by several regulatory and standardization agencies for extractive gas-sampling analysis. Many highly reactive species in the exhaust can be simultaneously measured by FTIR even below part-per-million levels, replacing several discrete analyzers which may require complicated calibration procedures.

Among the absorption techniques, direct absorption spectroscopy, cavity enhancement approaches and photoacoustic spectroscopy coupled with laser sources have been demonstrated to give sensitive and selective sensors for on-line and in-situ applications, with high sensitivity, compact set-up, fast time response and portability. Infrared tunable semiconductor lasers represent the ideal radiation sources for gas sensing thanks to their excellent spectroscopic and technical properties, i.e., narrow linewidth, tunability, reliability and room-temperature operation.

QEPAS represents an innovative laser based spectroscopic technique promising in commercial sensor for automotive applications thanks to good performances in terms of selectivity and sensitivity, compactness and ease of operation.

Metal Insulator Semiconductor field effect devices used as gas sensors can be of different types: transistors, Schottky diodes or capacitors, with transistors being preferred for commercial devices. The gas sensing principle for field effect sensors is based on molecules adsorbing and dissociating on a catalytically active gate material on the sensor. These interactions create a change in the electric charges on the semiconductor surface, which in turn results in a shift in the sensor output voltage. The interactions of the gas molecules with the gate material depend on the operating temperature and the morphology and chemical characteristics of the gate material.

The use of nanostructured films as gate material has the potential to give sensors with increased sensitivity, and faster response and recovery time, due to the larger surface area available for interaction with the gas molecules, as compared to conventional thin film sensing layers. The optimum sensor performance has not been fully realized due to limited understanding of the catalytic properties of the active layer, the active layer-gas interactions, the effects of processing techniques and experimental conditions; which do influence the microstructure, morphology, and electrical properties of the nanomaterials. Improvements have been seen for selectivity, but operation at high temperature is still an open issue.

## 5. Acknowledgment

Financial support from the Apulian District on Mechatronics (MEDIS) is gratefully acknowledged.

## 6. References

- Adachi, M. (2000). Emission measurement techniques for advanced powertrains. *Measurement Science and Technology*. Vol. 11, No. 10, (January 2000), pp. R113-R129, ISSN 0957-0233
- Ahn, M. -W.; Park, K. -S.; Heo, J. -H.; Kim, D. -W.; Choi, K. J. & Park, J. -G. (2009). On-chip fabrication of ZnO-nanowire gas sensor with high gas sensitivity. *Sensors and Actuators B*, Vol. 138, No. 1, (April 2009), pp. 168-173, ISSN 0925-4005
- Alving, K.; Weitzberg, E. & Lundberg, JM. (1993). Increased amount of nitric oxide in exhaled air of asthmatics. *European Respiratory Journal* Vol. 6, No. 9, (October 1993) pp. 1368-1370
- Aroutiounian, V. M. (2007). Semiconductor NO<sub>x</sub> sensors. *International Scientific Journal for Alternative Energy and Ecology*, Vol. 4, No. 48, (April 2007), pp. 63-76, ISSN 1608-8298
- Balazsi, C.; Sedlackova, K.; Llobet, E. & Ionescu, R. (2008). Novel hexagonal WO<sub>3</sub> nanopowder with metal decorated carbon nanotubes as NO<sub>2</sub> gas sensors. *Sensors and Actuators B*, Vol. 133, No. 1, (July 2008), pp. 151-155, ISSN 0925-4005
- Barsan, N.; Schweizer-Berberich, M. & Göpel, W. (1999). Fundamental and practical aspects in the design of nanoscaled SnO<sub>2</sub> gas sensors: a status report. *Fresenius Journal of Analytical Chemistry*, Vol. 365, No. 4, (October 1999), pp. 287-304, ISSN 0937-0633
- Broqvist, P.; Gronbeck, H.; Fridell, E. & Panas, I. (2004). NO<sub>x</sub> storage on BaO: theory and experiment. *Catalysis Today*, Vol. 96, No. 3, (October 2004), pp. 71-78, ISSN 0920-5861
- Carotta, M. C.; Cervi, A.; di Natale, V.; Gherardi, S.; Giberti, A.; Guidi, V.; Puzzovio, D.; Vendemiati, B.; Martinelli, G.; Sacerdoti, M.; Calestani, D.; Zappettini, A.; Zha, M. & Zanotti, L. (2009). ZnO gas sensors: a comparison between nanoparticles and nanotetrapods-based thick films. *Sensors and Actuators B*, Vol. 137, No. 1, (March 2009), pp. 164-169, ISSN 0925-4005
- Choi, K. J. & Jang, H. W. (2010). One-dimensional oxide nanostructures as gas-sensing materials: reviews and issues. *Sensors*, Vol. 10, No. 4, (April 2010), pp. 4083-4099, ISSN 1424-8220
- Cioffi, N.; Colaianni, L.; Ieva, E.; Pilolli, R.; Ditaranto, N.; Angione, M. D.; Cotrone, S.; Buchholt, K.; Spetz, A. L.; Sabbatini, L. & Torsi, L. (2011). Electrosynthesis and characterization of gold nanoparticles for electronic capacitance sensing of pollutants. *Electrochimica Acta*, Vol. 56, No. 10, (April 2011), pp. 3713-3720, ISSN 0013-4686
- Comini, E. & Sberveglieri, G. (2010). Metal oxide nanowires as chemical sensors. *Materials Today*, Vol. 13, No. 7-8, (Jul-Aug 2010), pp. 36-44, ISSN 1369-7021
- Di Franco, C.; Elia, A.; Spagnolo, V.; Scamarcio, G.; Lugarà, P.M.; Ieva, E.; Cioffi, N.; Torsi, L.; Bruno, G.; Losurdo, M.; Garcia, M.A.; Wolter, S.D.; Brown, A. & Ricco, M. (2009). Optical and electronic NO<sub>x</sub> sensors for applications in mechatronics. *Sensors*, Vol. 9, No. 5, (May 2009), pp. 3337-3356, ISSN 3337-3356
- Durbin, T. D.; Wilson, R. D.; Norbeck, J. M.; Wayne, J. M.; Huai, T. & Rhee, S. H. (2002). Estimates of the emission rates of ammonia from light-duty vehicles using standard chassis dynamometer test cycles. *Atmospheric Environment*, Vol. 36, No. 9, (January 2002), pp. 1475-1482, ISSN 1352-2310

- Elia, A.; Lugarà, P.M. & Giancaspro, C. (2005). Photoacoustic detection of nitric oxide by use of a quantum-cascade laser. *Optics Letters*, Vol. 30, No. 9, (May 2005), pp. 988-990, ISSN 1424-8220
- Elia, A.; Lugarà, P.M.; Di Franco, C. & Spagnolo, V. (2009). Photoacoustic Techniques for Trace Gas Sensing Based on Semiconductor Laser Sources. *Sensors*, Vol. 9, No. 12, (December, 2009 ), pp. 9616-9628, ISSN 1424-8220
- Elia, A.; Lugarà, P.M.; Di Franco, C. & Spagnolo, V. (2011). Quantum Cascade Laser Technology for the Ultrasensitive Detection of Low-Level Nitric Oxide, In: *Nitric Oxide - Methods and Protocols*, Helen O. O. McCarthy, Jonathan A. A. Coulter, pp. 115-133, Humana Press, ISBN: 978-1-61737-963-5
- EPA: Method 320 (1998) Measurement of vapor phase organic and inorganic emissions by extractive Fourier transform infrared (FTIR) spectroscopy, in: *Federal Register, Environmental Protection Agency, 40 CFR Part 63, Appendix A to Part 63-Test Methods*, pp. 14 219-14 228
- Faist, J.; Capasso, F.; Sivco, D. L.; Sirtori, C.; Hutchinson, A. L. & Cho, A. Y. (1994). Quantum cascade laser. *Science*, Vol. 264, No. 5158, (April 1994), pp. 553-556, ISSN 0036-8075.
- Fine, G. F.; Cavanagh, L. M.; Afonja, A. & Binions, R. (2010). Metal oxide semi-conductor gas sensors in environmental monitoring. *Sensors*, Vol. 10, No. 6, (June 2010), pp. 5469-5502, ISSN 1424-8220
- Firooz, A. A.; Hyodo, t.; Mahjoub, A. R.; Khodadi, A. A. & Shimizu, Y. (2010). Synthesis and gas sensing properties of nano- and meso-porous MoO<sub>3</sub>-doped SnO<sub>2</sub>. *Sensors and Actuators B*, Vol. 147, No. 2, (June 2010), pp. 554-560, ISSN 0925-4005
- Guo, Y.; Zhang, X. W. & Han, G. R. (2006) Investigation of structure and properties of N-doped TiO<sub>2</sub> thin films grown by APCVD. *Material Science and Engineering B*, Vol. 135, No. 2, (November 2006), pp. 83-87, ISSN 0925-4005
- Guo, Z.; Li, M. & Liu, J. (2008). Highly porous CdO nanowires: preparation based on hydroxyl- and carbonate- containing cadmium compound precursor nanowires, gas sensing and optical properties. *Nanotechnology*, Vol. 19, No. 24, (June 2008), pp. 245611, ISSN 0957-4484
- Gurlo, A.; Bârsan, N.; Ivanovskaya, M.; Weimar, U. & Göpel, W. (1998). In<sub>2</sub>O<sub>3</sub> and MoO<sub>3</sub>-In<sub>2</sub>O<sub>3</sub> thin film semiconductor sensors: interaction with NO<sub>2</sub> and O<sub>3</sub>. *Sensors and Actuators B*, Vol. 47, No. 1-3 (April 1998), pp. 92-99, ISSN 0925-4005
- Hanwell, M. D.; Heriot, S. Y.; Richardson, T. H.; Cowlam, N. & Ross, I. M. (2006). Gas and vapor sensing characteristics of Langmuir-Schaeffer thiol encapsulated gold nanoparticle thin films. *Colloids and Surfaces A*, Vol. 284-285, (August 2006), pp. 379-383, ISSN 0927-7757
- Hara, K.; Nakatani, S.; Rahman, M.; Nakamura, H.; Tanaka Y. & Ukon, J. (2009). Development of Nitrogen Components Analyzer Utilizing Quantum Cascade Laser". *SAE Technical Paper 2009-01-2743*, doi:10.4271/2009-01-2743
- Hoa, N. D.; Quy, N. V.; Cho, Y. & Kim, D. (2009b). Porous single wall carbon nanotube films formed by in situ arc-discharge deposition for gas sensors application. *Sensors and Actuators B*, Vol. 135, No. 2, (January 2009), pp. 656-663, ISSN 0925-4005
- Hoa, N. D.; Quy, N. V. & Kim, D. (2009a). Nanowire structured SnO<sub>x</sub>-SWNT composites: high performance sensor for NO<sub>x</sub> detection. *Sensors and Actuators B*, Vol. 142, No. 1, (October 2009), pp. 253-259, ISSN 0925-4005

- Hoa, N. D.; Quy, N. V.; Tuan, M. A. & Hieu, N. V. (2009c). Facile synthesis of p-type semiconducting cupric oxide nanowires and their gas sensing properties. *Physica E*, Vol. 42, No. 2, (December 2009), pp. 146-149, ISSN 1386-9477
- Hoch, P. K. (1992). The development of the band theory of solids, 1933-1960, In: *Out of the Crystal Maze – Chapters from the History of Solid State Physics*, Hoddeson, L.; Braun, E.; Teichmann, J.; Weart, S. (Eds.), pp. 182-235, Oxford University Press, ISBN 978-0-19-505329-6, New York, USA
- Horiba (2010) Vehicle Test Systems. 04/18/2011 Available from:  
<<http://www.horiba.com/it/automotive-test-systems>>
- Hwang, H. -S.; Song, J. -T.; Yeo, D. -H.; Shin, H. -S.; Hong, Y. -W.; Kim, J. -H. & Lim, D. G. (2008). Characteristics of a NO<sub>x</sub> gas sensor based on a low temperature co-fired ceramic and Ga-doped ZnO. *Journal of the Korean Physical Society*, Vol. 53, No. 3, (September 2008), pp. 1384-1387, ISSN 0374-4884
- Ieva, E.; Buchholt, K.; Colaianni, L.; Cioffi, N.; Sabbatini, L.; Capitani, G. C.; Spetz, A. L.; Kall, P. O. & Torsi, L. (2008). Au nanoparticles as gate material for NO<sub>x</sub> field effect capacitive sensors. *Sensors Letters*, Vol. 6, No. 1, (February 2008), pp. 1-8, ISSN 1546-1971
- Jun, J. H.; Yun, J.; Cho, K.; Hwang, I. -S.; Lee, J. -H. & Kim, S. (2009). Necked ZnO nanoparticle -based NO<sub>2</sub> sensors with high and fast response. *Sensors and Actuators B*, Vol. 140, No. 2, (July 2009), pp. 412-417, ISSN 0925-4005
- Kannan, S.; Rieth, L. & Solzbacher, F. (2010a). NO<sub>x</sub> sensitivity of In<sub>2</sub>O<sub>3</sub> thin film layers with and without promoter layers at high temperatures. *Sensors and Actuators B*, Vol. 149, No. 1, (August 2010), pp. 8-19, ISSN 0925-4005
- Kannan, S.; Steinebach, H.; Rieth, L. & Solzbacher, F. (2010b). Selectivity, stability and repeatability of In<sub>2</sub>O<sub>3</sub> thin films towards NO<sub>x</sub> at high temperatures (>500°C). *Sensors and Actuators B*, Vol. 148, No. 1, (June 2010), pp. 126-134, ISSN 0925-4005
- Kasyutich, V.L., Holdsworth, R.J. & Martin, P.A. (2009). In situ vehicle engine exhaust measurements of nitric oxide with a thermoelectrically cooled, cw DFB quantum cascade laser. *Journal of Physics: Conference Series*, Vol. 157, No. 1, (January 2009), pp. 1-6, ISSN 1742-6596
- Kida, T.; Nishiyama, A.; Yuasa, M.; Shimanoe, K. & Yamazoe, N. (2009). Highly sensitive NO<sub>2</sub> sensors using lamellar-structured WO<sub>3</sub> particles prepared by an acidification method. *Sensors and Actuators B*, Vol. 135, No. 2, (January 2009), pp. 568-574, ISSN 0925-4005
- Ko, G.; Kim, H. -Y.; Ahn, J.; Park, Y. -M.; Lee, K. -Y. & Kim, J. (2010). Graphene-based nitrogen dioxide gas sensors. *Current Applied Physics*, Vol. 10, No. 4, (July 2010), pp. 1002-1004, ISSN 1567-1739
- Kong, F.; Wang, Y.; Zhang, J.; Xia, H.; Zhu, B.; Wang, Y.; Wang, S. & Wu, S. (2008). The preparation and gas sensitivity study of polythiophene-SnO<sub>2</sub> composites. *Material Science and Engineering B*, Vol. 150, No. 1, (April 2008), pp. 6-11, ISSN 0925-4005
- Kosterev A.A., & Tittel F. (2002a). Chemical sensors based on quantum cascade lasers. *IEEE Journal of Quantum Electronics*, Vol. 38, No. 6, (June 2002), pp. 582-591, ISSN: 0018-9197

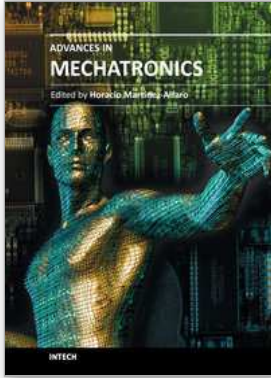
- Kosterev, A.A.; Bakhirkin, Y.A.; Curl, R.F. & Tittel, F.K. (2002b). Quartz-enhanced photoacoustic spectroscopy. *Optics Letters*, Vol. 27, No. 21, (November 2002), pp. 1902-1904, ISSN 0146-9592
- Kosterev, A.A.; Tittel, F.K.; Serebryakov, D.; Malinovsky, A. & Morozov, A. (2005). Applications of quartz tuning fork in spectroscopic gas sensing. *Review of Scientific Instruments*, Vol. 76, (March 2005), pp. 0431051- 0431059, ISSN 0034-6748
- Kupriyanov, L. Y. (1996). Semiconductor sensors in physico-chemical studies, In: *Handbook of Sensors and Actuators, Vol. 4*, Middelhoek, S. (Ed.), pp. 1-400, Elsevier Science B. V., ISBN 0-444-82261-5, Amsterdam, The Netherlands
- Lee, J. -H. (2009). Gas sensors using hierarchical and hollow oxide nanostructures: overview. *Sensors and Actuators B*, Vol. 140, No. 1, (June 2009), pp. 319-336, ISSN 0925-4005
- Leghirib, R.; Pavalko, R.; Felten, A.; Vasiliev, A.; Cane, C.; Gracia, I.; Pireaux, J. & Llobet, E. (2010). Gas sensors based on multi-wall carbon nanotubes decorated with tin oxide nanoclusters. *Sensors and Actuators B*, Vol. 145, No. 1, (March 2010), pp. 411-416, ISSN 0925-4005
- Lin, C. Y.; Fang, Y. -Y.; Lin, C. -W.; Tunney, J. J. & Ho, K. -C. (2010). Fabrication of NO<sub>x</sub> gas sensors using In<sub>2</sub>O<sub>3</sub>-ZnO composite films. *Sensors and Actuators B*, Vol. 146, No. 1, (April 2010), pp. 28-34, ISSN 0925-4005
- Lou, X. W.; Archer, L. A. & Yang, Z. (2008). Hollow micro-/nanostructures: synthesis and applications. *Advanced Materials*, Vol. 20, No. 21, (September 2008), pp. 3987-4019, ISSN 0935-9648
- Mandelis, A. & Christofides, C. (1993). *Physics, Chemistry and Technology of Solid State Gas Sensor Devices*, John Wiley & Sons, Inc., ISBN 0-471-55885-0, New York, USA
- Marinelli, F.; Dell'Aquila, A.; Torsi, L.; Tey, J.; Suranna, G. P.; Mastrorilli, P.; Romanazzi, G.; Nobile, C. F.; Mhaisalkar, S. G.; Cioffi, N. & Palmisano, F. (2009). An organic field effect transistor as a selective NO<sub>x</sub> sensor operated at room temperature. *Sensors and Actuators B*, Vol. 140, No. 2, (July 2009), pp. 445-450, ISSN 0925-4005
- McCulloch, M.T.; Langford, N. & Duxbury, G. (2005). Real-time trace-level detection of carbon dioxide and ethylene in car exhaust gases. *Applied Optics*, Vol. 44, No. 14, (May 2005) pp. 2887-2894, ISSN 1559-128X
- Naso, F.; Babudri, F.; Colangiuli, D.; Garinola, G. M.; Quaranta, F.; Rella, R.; Tafuro, R. & Valli, L. (2003). Thin film construction and characterization and gas sensing performances of a tailored phenylene-thienylene copolymer. *Journal of the American Chemical Society*, Vol. 125, No. 30, (July 2003), pp. 9055-9061, ISSN 0002-7863
- Navale, S. C.; Ravi, V. & Mulla, I. S. (2009). Investigations on Ru-doped ZnO: strain calculations and gas sensing study. *Sensors and Actuators B*, Vol. 139, No. 2, (June 2009), pp. 466-470, ISSN 0925-4005
- Nakamura H.; Haga I.; & Murakami K. (2006). Trend of Exhaust Emission Standards for Diesel-Powered Vehicles. *RTRI Report (Railway Technical Research Institute)*, Vol. 20, No. 7, pp. 53-56, ISSN:0914-2290
- Nomani, M. W. K.; Shishir, R.; Qazi, M.; Diwan, D.; Shields, V. B.; Spencer, M. G.; Tompa, G. S.; Sbrockey, N. M. & Koley, G. (2010). Highly sensitive and selective detection of NO<sub>2</sub> using epitaxial graphene on 6H-SiC. *Sensors and Actuators B*, Vol. 150, No. 1, (September 2010), pp. 301-307, ISSN 0925-4005

- Novoselov, K. S.; Geim, A. K.; Morozov, S. V.; Jiang, D.; Zhang, Y.; Dubonos, S. V.; Grigorieva, I. V. & Firsov, A. A. (2004). Electric field effect in atomically thin carbon films. *Science*, Vol. 306, No. 5696, (October 2004), 666-669, ISSN 0036-8075
- Oh, E.; Choi, H. -Y.; Jung, S. -H.; Cho, S.; Kim, J. C.; Lee, K. -H.; Kang, S. -W.; Kim, J.; Yun, J. -Y. & Jeong, S. -H. (2009). High performance NO<sub>2</sub> gas sensor based on ZnO nanorod grown by ultrasonic irradiation. *Sensors and Actuators B*, Vol. 141, No. 1, (August 2009), pp. 239-243, ISSN 0925-4005
- O'Keefe, A. & Deacon D.A. G. (1988). Cavity ring-down optical spectrometer for absorption measurements using pulsed laser sources. *Review of Scientific Instruments*, Vol. 59, (December 1988), pp. 2544-2551, ISSN 0034-6748
- Oprea, A.; Frerichs, H. -P.; Wilbertz, C.; Lehmann, M. & Weimar, U. (2007). Hybrid gas sensor platform based on capacitive coupled field effect transistors: ammonia and nitrogen dioxide detection. *Sensors and Actuators B*, Vol. 127, No. 1, (October 2007), pp. 161-167, ISSN 0925-4005
- Park, J. -A.; Moon, J.; Lee, S. -J.; Kim, S. H.; Chu, H. Y. & Zyung, T. (2010). SnO<sub>2</sub>-ZnO hybrid nanofibers-based highly sensitive nitrogen dioxide sensors. *Sensors and Actuators B*, Vol. 145, No. 1, (March 2010), pp. 592-595, ISSN 0925-4005
- Qin, Y.; Hu, M. & Zhang, J. (2010). Microstructure characterization and NO<sub>2</sub> sensing properties of tungsten oxide nanostructures. *Sensors and Actuators B*, Vol. 150, No. 1, (September 2010), pp. 339-345, ISSN 0925-4005
- Reyes F.; Grutter M.; Jazcilevich A. & Gonz'alez-Oropeza R. (2006). Analysis of non-regulated vehicular emissions by extractive FTIR spectrometry: tests on a hybrid car in Mexico City. *Atmospheric Chemistry and Physics*, Vol. 6, No. 4, (November 2006), pp. 5339-5346
- Sayago, I.; Santos, H.; Horrillo, M. C.; Aleixandre, M.; Fernandez, M. J.; Derrado, E.; Tacchini, I.; Aroz, R.; Maser, W. K.; Benito, A. M.; Martinez, M. T.; Gutierrez, J. & Munoz, E. (2008). Carbon nanotube networks as gas sensors for NO<sub>2</sub> detection, *Talanta*, Vol. 77, No. 2, (December 2008), pp. 758-764, ISSN 0039-9140
- Sberveglieri, G. (1992). *Gas Sensors: Principles, Operation and Developments*, Kluwer Academic Publishers, ISBN 0-7923-2004-2, Dordrecht, The Netherlands
- Shen, G.; Chen, P. -C.; Ryu, K. & Zhou, C. (2009). Devices and chemical sensing applications of metal oxide nanowires. *Journal of Materials Chemistry*, Vol. 19, No. 7, (July 2009), pp. 828-839, ISSN 0959-9428
- Shouli, B.; Liangyuan, C.; Dianqing, L.; Wensheng, Y.; Pengcheng, Y.; Zhiyong, L.; Aifan, C. & Liu, C. C. (2010). Different morphologies of ZnO nanorods and their sensing property. *Sensors and Actuators B*, Vol. 146, No. 1, (April 2010), pp. 129-137, ISSN 0925-4005
- Shu, J. H.; Wickle, H. C.; Chin, B. A. (2010). Passive chemiresistor sensor based on iron (II) phthalocyanine thin films for monitoring of nitrogen dioxide. *Sensors and Actuators B*, Vol. 148, No. 2, (July 2010), pp. 498-503, ISSN 0925-4005
- Seiyama, T.; Kato, A.; Fujiiishi, K.; Nagatani, M. (1962). A new detector for gaseous components using semiconductive thin films. *Analytical Chemistry*, Vol. 34, No. 11, (October 1962), pp. 1502-1503, ISSN 0003-2700

- Seinfeld J.H. & S.N. Pandis (1998). Atmospheric Chemistry and Physics, In: *From Air Pollution to Climate Change*, John Wiley & Sons, ISBN: 9780471178163, New York (NY), USA
- Spagnolo, V.; Kosterev, A.A.; Dong, L.; Lewicki, R. & Tittel, F.K. (2010). NO trace gas sensor based on quartz-enhanced photoacoustic spectroscopy and external cavity quantum cascade laser. *Applied Physics B*, Vol. 100, No. 1, (July 2010), pp. 125–130, ISSN 0946-2171
- Sumizawa, H.; Yamada, H. & Tonokura, K. (2010). Real-time monitoring of nitric oxide in diesel exhaust gas by mid-infrared cavity ring-down spectroscopy. *Applied Physics B*, Vol. 100, No. 4, (July 2010), pp. 925–931, ISSN: 0946-2171
- Sze, S. M. (1994). *Semiconductor Sensors*, John Wiley & Sons, Inc., ISBN 0-471-54609-7, New York, USA
- Thermo Fisher Scientific Inc. (2007). The Use of FT-IR to Analyze NO<sub>x</sub> Gases in Automobile Exhaust, In: *Application Note: 50649*. 04/18/2011, Available from: [https://www.thermo.com/eThermo/CMA/PDFs/Articles/articlesFile\\_7219.pdf](https://www.thermo.com/eThermo/CMA/PDFs/Articles/articlesFile_7219.pdf)
- Tingvall, B.; Pettersson, E. & Agren, E. (2007). Vehicle test system - A pilot study, In: *Luleå University of Technology Department of Human Work Sciences Division of Sound and Vibration - Technical Report*, 04/18/2011, Available from: <http://epubl.ltu.se/1402-1536/2007/11/LTU-TR-0711-SE.pdf>
- Tricoli, A.; Righettoni, M. & Teleki, A. (2010). Semiconductor gas sensors: dry synthesis and applications. *Angewandte Chemie International Edition*, Vol. 49, No. 46, (October 2010), pp. 7632-7659, ISSN 1433-7851
- Ueda, T.; Bhuiyan, M. M. H.; Norimatsu, H.; Katsuki, S.; Ikegami, T. & Mitsugi, F. (2008). Development of carbon nanotube based gas sensors for NO<sub>x</sub> gas detection working at low temperature. *Physica E*, Vol. 40, No. 7, (May 2008), pp. 2272-2277, ISSN 1386-9477
- Van Asselt H. & Biermann, F. (2007). European emissions trading and the international competitiveness of energy-intensive industries: a legal and political evaluation of possible supporting measures. *Energy Policy*, Vol. 35, No.1, (January 2007), pp. 497-506
- Wang, C. Y.; Ali, M.; Kups, T.; Rohlig, C. -C.; Cimella, V.; Stauden, T. & Ambacher, O. (2008). NO<sub>x</sub> sensing properties of In<sub>2</sub>O<sub>3</sub> nanoparticles prepared by metal organic chemical vapor deposition. *Sensors and Actuators B*, Vol. 130, No. 2, (March 2008), pp. 589-593, ISSN 0925-4005
- Weber, W.H.; Remillard, J.T.; Chase, R.E.; Richert, J.F.; Capasso, F.; Gmachl, C.; Hutchinson, A.L.; Sivco, D.L.; Baillargeon, J.N. & Cho, A.Y. (2002). Using a Wavelength-Modulated Quantum Cascade Laser to Measure NO Concentrations in the Parts-per-Billion Range for Vehicle Emissions Certification. *Applied Spectroscopy*, Vol. 56, No. 6, (June 2002), pp. 706-714, ISSN 0003-7028
- Wei, B. Y.; Hsu, M. C.; Su, P. G.; Lin, H. M.; Wu, R. J. & Lai, H. J. (2004). A novel SnO<sub>2</sub> gas sensors doped with carbon nanotubes operating at room temperature. *Sensors and Actuators B*, Vol. 101, No. 1-2, (June 2004), pp. 81-89, ISSN 0925-4005
- Williams, D. E. (1999). Semiconducting oxides as gas-sensitive resistors. *Sensors and Actuators B*, Vol. 57, No. 1-3, (September 1999), pp. 1-19, ISSN 0925-4005

- Yamazoe, N.; Fuchigami, J.; Kishikawa, M. & Seiyama, T. (1979). Interactions of tin oxide surface with O<sub>2</sub>, H<sub>2</sub>O and H<sub>2</sub>. *Surface Science*, Vol. 86, (July 1979), pp. 335-344, ISSN 0039-6025
- Zhang, C.; Debliquy, M.; Boudiba, A.; Liao, H. & Coddet, C. (2010). Sensing properties of atmospheric plasma sprayed WO<sub>3</sub> coating for sub ppm NO<sub>2</sub> detection. *Sensors and Actuators B*, Vol. 144, No. 1, (January 2010), pp. 282-288, ISSN 0925-4005
- Zhang, J.; Wang, S.; Wang, Y.; Wang, Y.; Zhu, B.; Xia, H.; Guo, X.; Zhang, S.; Huang, W. & Wu, S. (2009). NO<sub>2</sub> sensing performance of SnO<sub>2</sub> hollow-sphere sensor. *Sensors and Actuators B*, Vol. 135, No. 2, (January 2009), pp. 610-617, ISSN 0925-4005





## **Advances in Mechatronics**

Edited by Prof. Horacio Martinez-Alfaro

ISBN 978-953-307-373-6

Hard cover, 300 pages

**Publisher** InTech

**Published online** 29, August, 2011

**Published in print edition** August, 2011

Numerous books have already been published specializing in one of the well known areas that comprise Mechatronics: mechanical engineering, electronic control and systems. The goal of this book is to collect state-of-the-art contributions that discuss recent developments which show a more coherent synergistic integration between the mentioned areas. The book is divided in three sections. The first section, divided into five chapters, deals with Automatic Control and Artificial Intelligence. The second section discusses Robotics and Vision with six chapters, and the third section considers Other Applications and Theory with two chapters.

### **How to reference**

In order to correctly reference this scholarly work, feel free to copy and paste the following:

Angela Elia, Cinzia Di Franco, Adeel Afzal, Nicola Cioffi and Luisa Torsi (2011). Advanced NOx Sensors for Mechatronic Applications, Advances in Mechatronics, Prof. Horacio Martinez-Alfaro (Ed.), ISBN: 978-953-307-373-6, InTech, Available from: <http://www.intechopen.com/books/advances-in-mechatronics/advanced-nox-sensors-for-mechatronic-applications>

**INTECH**  
open science | open minds

### **InTech Europe**

University Campus STeP Ri  
Slavka Krautzeka 83/A  
51000 Rijeka, Croatia  
Phone: +385 (51) 770 447  
Fax: +385 (51) 686 166  
[www.intechopen.com](http://www.intechopen.com)

### **InTech China**

Unit 405, Office Block, Hotel Equatorial Shanghai  
No.65, Yan An Road (West), Shanghai, 200040, China  
中国上海市延安西路65号上海国际贵都大饭店办公楼405单元  
Phone: +86-21-62489820  
Fax: +86-21-62489821

© 2011 The Author(s). Licensee IntechOpen. This chapter is distributed under the terms of the [Creative Commons Attribution-NonCommercial-ShareAlike-3.0 License](#), which permits use, distribution and reproduction for non-commercial purposes, provided the original is properly cited and derivative works building on this content are distributed under the same license.